Ninth Canadian Conference on
Earthquake Engineering
Ottawa, Ontario, Canada
26-29 June 2007

A DISPLACEMENT-BASED EVALUATION APPROACH FOR ANALYSIS OF REINFORCED CONCRETE BUILDINGS INFILLED WITH MASONRY PANELS

H. Mostafaei[1] and T. Kabeyasawa[2]

ABSTRACT

An analytical process was modified for a displacement-based analysis of reinforced concrete buildings infilled with masonry panels. Frame-panel interaction was considered by applying an equivalent compression strut width for the masonry panel. The model was verified by the results of an experimental study conducted in University of Tokyo. As an example of the application of the approach, the Bam Telephone Center infill masonry reinforced concrete building of Iran, constructed shortly before the 2003 Bam Earthquake, was modeled using this approach and simulated under the strong motion record. The results of three-dimension nonlinear dynamic analysis were compared with the cracks and damages inspection, which was observed after the earthquake. A satisfactory correlation was obtained for the results of these comparisons.

Introduction

For many years, structural engineers, in the design process of structures such as buildings, have typically ignored the effects of infill masonry walls in the structural analysis. In other words, the structures have been analyzed based on the bare frames. In the last four decades, the effect of infill walls in frame structures has been extensively studied. Experimental and analytical study results show that infill walls have a significant effect on both stiffness and strength of structures (Moghaddam and Dowling, 1987). Studies have also been done to obtain analytical models for considering the effect of infill walls in the analysis (Madan et al. 1997). Later, an analytical procedure for structural analysis was presented for application in practice (Mostafaei and Kabeyasawa 2004). In the latter study, post-peak response was modeled based on previous experimental data. To ensure applicability of the model for concrete block infill masonry walls, common in Japan, an experimental study was carried out and the proposed model was verified by the test data (Mostafaei 2006). In this article, the modified infill masonry wall model and analytical process as well as the Bam building case study are presented.

Analytical Modeling of Frame Infilled with Masonry Wall

Analytical steps for a frame with infill masonry walls are described here when the structure is subjected to seismic load combined with dead load and live load. Since, in most cases, the effect of vertical seismic

[1]Postdoctoral Fellow, Dept. of Civil Engineering, University of Toronto, Toronto, ON, M5S 1A4 Canada
[2]Professor, Earthquake Research Institute, University of Tokyo, Tokyo, 113-0032 Japan

load can be ignored in the analysis, only lateral stiffness of the masonry infill walls are taken into account to compute the structural stiffness. Hence, masonry panel is modeled as a single horizontal spring working parallel with the corresponding frame stiffness. Even for infill panels with openings, an equivalent single spring is determined to interact with the frame. This reduces the analytical errors due to convergence quandary in the nonlinear stage.

Masonry Infill Wall Model

A masonry infill panel is modeled by replacing the panel by a single horizontal spring. However, force displacement relationship of the spring is derived from force-displacement relationship of a diagonal masonry compression strut model. By ignoring the tensile strength of the infill masonry and considering a reverse lateral loading system, the same force-displacement relationship can be applied for the negative lateral direction. Fig. 1 illustrates the analytical model as well as force-displacement envelope for the masonry infill wall model. The main factors of the envelope model, in Fig. 1, are shear strengths at the assumed yielding point, Vy , at the maximum point Vm, and the post-peak residual shear strength, Vp, and their corresponding displacements, Uy, Um, and Up, respectively. In the figure, α is the ratio of stiffness after yielding to that of the initial stiffness.

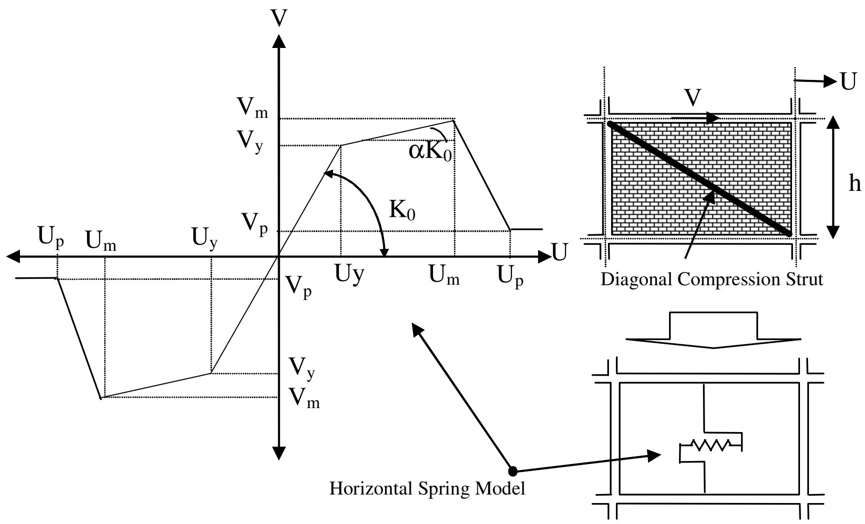

Figure 1. Analytical model for conventional masonry infill walls.

In order to obtain the main parameters of the envelope curve, first maximum lateral strength, V_m, is estimated by considering two failure modes, sliding shear and compression failures, described in the next section. Other factors can be determined based on the maximum lateral strength, V_m, and following equations. Maximum displacement at the maximum lateral force is estimated by Eq. 1, (Madan et al. 1997):

$$U_m = \frac{\varepsilon'_m d_m}{\cos\theta} \tag{1}$$

where, ε'_m is the masonry compression strain at the peak compression strength, and d_m is the diagonal strut length. A maximum drift limitation of 0.8% is applied for U_m/h_m ratio, which is derived from experimental results, (Mehrabi et al. 1996 and Chen 2003). h_m and θ are shown in Fig. 2. The initial stiffness K_0 can be estimated by the following equation.

$$K_0=2(V_m/U_m) \tag{2}$$

Lateral yielding force V_y, and displacement U_y may be calculated from the geometry in Fig. 1:

$$V_y = \frac{V_m - \alpha K_0 U_m}{1-\alpha} \tag{3}$$

$$U_y = \frac{V_y}{K_0} \tag{4}$$

Value of α is assumed equal to 0.2 for conventional concrete or solid brick infill walls.

U_p and V_p are defined based on the previews experimental results. The average value of drifts ratio at the 80% post-peak point, defined as a point on the envelope curve in Fig. 1 with shear level 80% of the maximum shear strength, is about 1.5% for concrete block infill walls, (Mehrabi et al. 1996) and (3/4)1.5%=1%, for solid bricks walls. The *Vp* and *Up* should be determined considering that the line connecting the peak of the envelope and the point (*Vp, Up*) passes through the 80% post-peak point. Therefore: Assuming,

$$Vp = 0.3\ Vm \tag{5}$$

Hence,

$$Up = 3.5ah_m - 2.5U_m \tag{6}$$

where, a= 0.01 for solid brick walls and a=0.015 for concrete block walls

Maximum Shear Strength of Infill Walls V_m

Failure modes of masonry walls can be categorized as sliding shear failure, horizontally, compression failure of the diagonal strut, diagonal tensile cracking and tension failure, flexural, (Paulay and Priestley 1992). The last two failure modes are not usually a critical failure mode for infill masonry walls.

Sliding Shear Failure

Sliding shear capacity of masonry wall is determined based on the Mohr-Coulomb failure criteria, which results in the following equation.

$$V_f = \frac{\tau_o t l_m}{(1-\mu \tan\theta)} \tag{7}$$

where, τ_o = cohesive capacity of the mortar beds, typically, $\tau_o = 0.04 f'_m$, (Paulay and Priestley, 1992), f'_m = Masonry compression strength, μ = sliding friction coefficient along the bed joint which is obtained by Eq. 8, (Chen 2003), t= infill wall thickness, and l_m = length of infill panel, shown in Fig. 2.

$$\mu = 0.654 + 0.000515 f'_j \tag{8}$$

where, f'_j is the mortar compression strength.

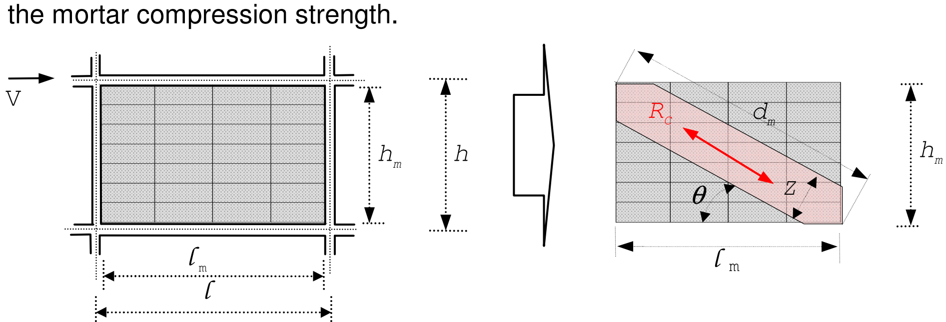

Figure 2. Infill masonry walls and the equivalent diagonal compression strut parameters.

Compression failure

Shear capacity of infill walls due to compression failure are computed based on compression strength of the wall strut.

$$V_c = ztf'_m \cos\theta \tag{9}$$

where, f'_m = Masonry compression strength, z= equivalent strut width obtained by Eq. 10, derived from paper by Stafford and Carter (Stafford and Carter 1969).

$$z = 0.175(\lambda h)^{-0.4} d_m \tag{10}$$

where, $\lambda = \left[\dfrac{E_m t \sin 2\theta}{4E_c I_g h_m}\right]^{\frac{1}{4}}$, in which h = column height between centerlines of beams, cm, h_m = height of infill panel, cm, E_c = modulus of elasticity of frame material, E_m = modulus of elasticity of infill material, $= 750 f'_m$, (Paulay and Priestley 1992), I_g = moment of inertial of column, cm^4, d_m = diagonal length of infill panel, cm, t = thickness of infill panel and equivalent strut, cm, and θ = angle whose tangent is the infill height-to-length aspect ratio, as: $\theta = \tan^{-1}\left(\dfrac{h_m}{l_m}\right)$ where, l_m= length of infill panel

Maximum shear strength of masonry wall should be limited by Eq. 11, recommended by ACI 530-88.

$$V_{max}/tl_m = 8.3 \quad kg/cm^2 \tag{11}$$

Modeling of Masonry Infill Wall with Openings

An equivalent spring model can be developed for infill wall with openings, (Mostafaei and Kabeyasawa 2004). To get properties of the equivalent model, first, infill wall is divided into partitions each modeled by a spring. Then a nonlinear pushover analysis is carried out for the frame with multiple springs and the result of force-displacement is derived as the envelope curve for the equivalent spring Se, shown in Fig. 3. Later, the acquired equivalent spring *Se* is employed as the infill wall model of the corresponding frame when modeling the entire structure.

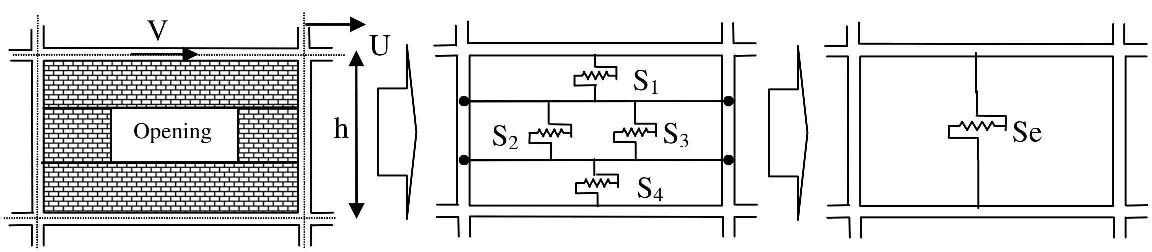

Figure 3. Equivalent spring model for infill masonry walls with openings.

Experimental Study

A reinforced concrete frame infilled with masonry wall, scaled 1/3 from a 6-strory building, was tested under varying axial load and cyclic lateral load, as shown in Fig. 4 (Mostafaei 2006). Masonry wall was modeled based on the process described in this article and considered as a shear spring in parallel with the frame, as shown in Fig.1. Applying Axial-Shear-Flexural-Interaction (ASFI) method (Mostafaei 2006), force-displacement of the bare frame was obtained and combined with the results of the masonry model.

Then the results of the analysis and the experimental data were compared and a satisfactory correlation was achieved.

Specimen Details and Material Properties

A reinforced concrete frame with concrete block wall, RCF+CBW, was tested in the structural laboratory of Earthquake Research Institute at The University of Tokyo. Reinforced concrete hollow block wall, with thickness of 70mm and a light amount of reinforcement; D6@ 400 vertically and D4@ 400 horizontally, was erected within the frame, one month after casting concrete of the RC frame. The steel bars were anchored by AE-Chemical Setter adhesive into the boundary columns

The two columns of the frame specimen have cross-section of 250mm×250mm and height of 1400mm. Table 1 gives details of the main bars and transverse reinforcement properties of the two columns. Top and bottom stubs have section of 500mm×400mm with 8-D19 as main bars and 4D10@100 as hoops.

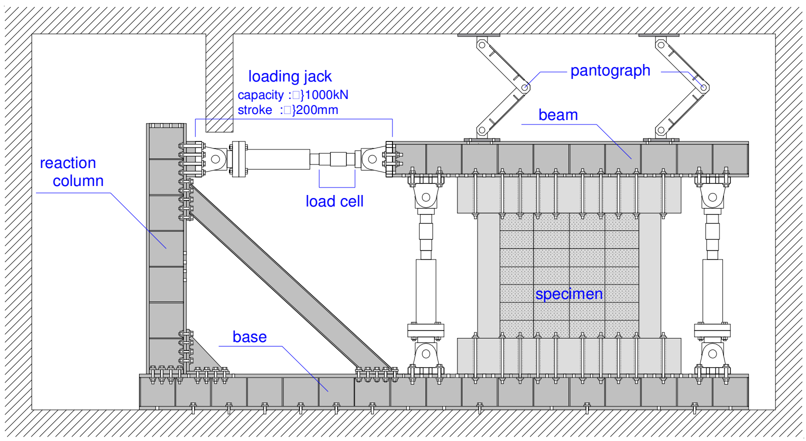

Figure 4. Test and Loading setup of specimen RCF+CBW.

Table 1. Reinforcement of columns.

Type	Yielding strength (MPa)	Reinforcement ratio %	Bars
Main Bars	385	1.82	16-D10
Hoops	330	0.10	D4@100

Table 2. Concrete of column and mortar of wall properties.

Samples	Compression strength MPa	Strain at the peak stress	Average tensile strength MPa
Concrete cylinder for columns and stubs (D=100mm, L=200mm)	21.4	0.002	2.2
Mortar cylinder (D=50mm, L=100mm)	42	0.0024	2.9

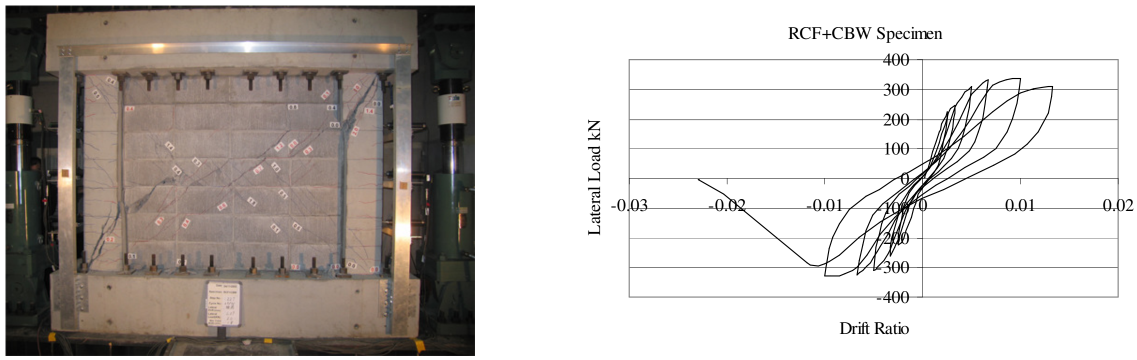

Figure 5. Specimen after failure and test result of top lateral load-drift ratio curve.

Table 2 shows cylinder compression test results for both concrete of columns and mortar of the wall. Compression test was carried out for hollow concrete blocks and an average of 15MPa was measured for the compression strength. The specimen configuration after failure and test results of top lateral load-drift ratio curve are shown in Fig.5.

Comparison of Experimental and Analytical Results

Based on the analytical method described in this paper, lateral force-displacement envelope curve of the specimen was estimated and illustrated in Fig. 6.

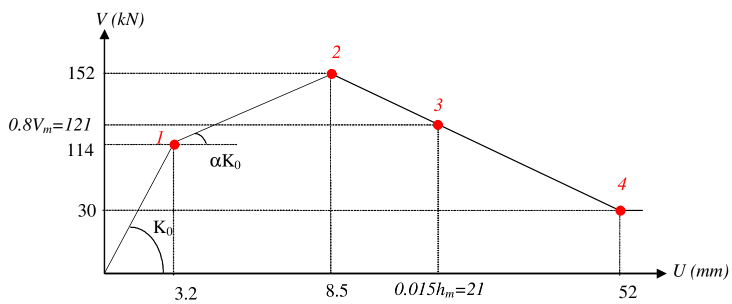

Figure 6. Force-displacement envelope curve for infill wall of specimen RCF-CBW.

On the other hand, lateral force- drift ratio response of the bare frame was evaluated based on ASFI method. Left sketch in Fig. 7 illustrates both results for the bare frame and the infill wall. The right sketch shows the combined analytical result for the frame with infill wall.

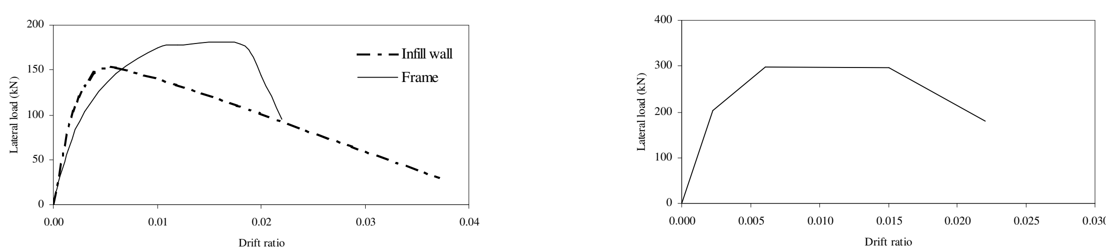

Figure 7. Drift ratio-lateral load response; *Left curve:* Individual response of bare frame and infill wall, *Right curve:* Combined results.

Comparison of the analytical and experimental results for the specimen is depicted in Fig. 8. Consistent results were achieved for stiffness, ultimate strength and deformations comparing to the experimental data. However, 10% lower maximum load was obtained by the analysis, which might be due to effects of varying axial load applied on the columns.

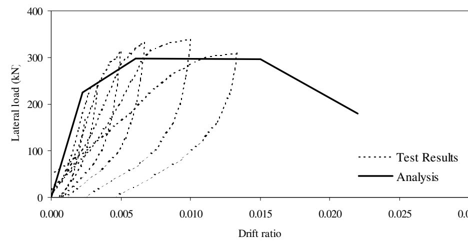

Figure 8. Comparison of test and analytical results for specimen RCF+CBW.

A Case Study on Seismic Response of Bam-Telephone-Center Reinforced Concrete Frame Building with Masonry Infill Walls Subjected to the 2003 Bam Earthquake

A reinforced concrete frame building, a telephone center, with infill masonry walls constructed in Bam city of Iran, was selected for detailed analysis by the analytical method, described in this paper. Bam telephone center building was a new building when the 2003 earthquake occurred in the region. One month after the earthquake, the author as a representative of the MEXT, Ministry of Education, Culture, Sport, Science and Technology of Japan was dispatched to the area in order to investigate on the building damages in Bam city of Iran and the villages nearby. A comprehensive survey was implemented, gathering information about 624 damaged buildings in the area (Mostafaei and Kabeyasawa 2004). Among those buildings, Bam telephone center was selected for more detailed investigation on the structural performance due to the earthquake. Bam telephone center building is a three-story nonsymmetrical reinforced concrete building, constructed just before the earthquake and located on Zeid square, N29.10^{o} and E58.37^{o} (about 1.5 km North-East of Bam strong motion station, installed by BHRC, Building and Housing Research Center of Iran). The peripheral and some of the internal frames of the building are infilled with masonry solid brick walls. Fig. 9 shows the overall building façade view and damages on the infill masonry walls and façade walls. The photos were taken one month after the earthquake. Infill masonry walls were observed with some diagonal and horizontal residual cracks. In the first floor, infill walls suffered higher level of damages and cracks comparing to the masonry walls in the basement and second floor. This might be due to the lower rate of infill walls in the first floor comparing to the other two floors. Alternatively, almost no damage or residual crack was observed on the structural elements, which might imply that the structure had almost linear performance during the earthquake. Based on the minimum base shear coefficient required by Iranian seismic design code for such a building, this building might not perform linearly subjected to the strong motion. Therefore a more close survey was carried out to evaluate the performance of the building

Figure 9. Bam telephone center reinforced concrete building after Dec. 2003 earthquake

Three-Dimensional Nonlinear Time-History Analysis

The computational model of the building is developed using the modeling capabilities of the software framework of OpenSees (Mazzoni S. et al. 2004). The building was modeled in the three-dimensional idealization. Linear shear force-deformation relationship is chosen for columns, relying on the fact that flexural failure occurs prior to shear failure, (also since no shear crack was observed on the columns and beams). All columns are modeled by the fiber element discretization, with four integration points. Infill masonry walls are modeled, individually, based on an equivalent horizontal zero-length element, as described in this article earlier. Damping characteristic of the building is modeled, applying mass and stiffness proportional damping with 5% of critical damping for the first two modes of vibration. The first two natural periods of the building are estimated using an eigen-value analysis applying the initial elastic stiffness matrix. The two natural periods are 0.41 and 0.40 seconds for the building with infill walls and 0.7 and 0.5 seconds for the bare frame. The East-west, EW, direction of the building is subjected to the east-west component of Bam strong motion record, E-W in Fig. 10, and north-south, NS, direction of the building is subjected to the north-south component of the record, N-S in Fig. 10.

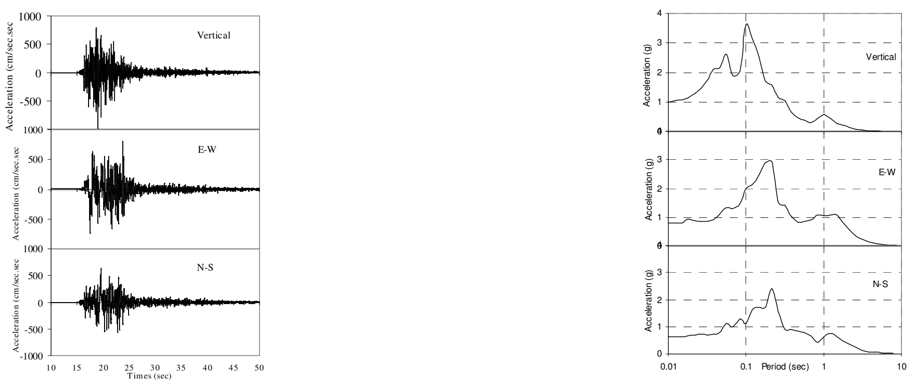

Figure 10. Three components of strong ground motion (left figures) and response spectra (right figure) of the 2003 Bam Earthquake.

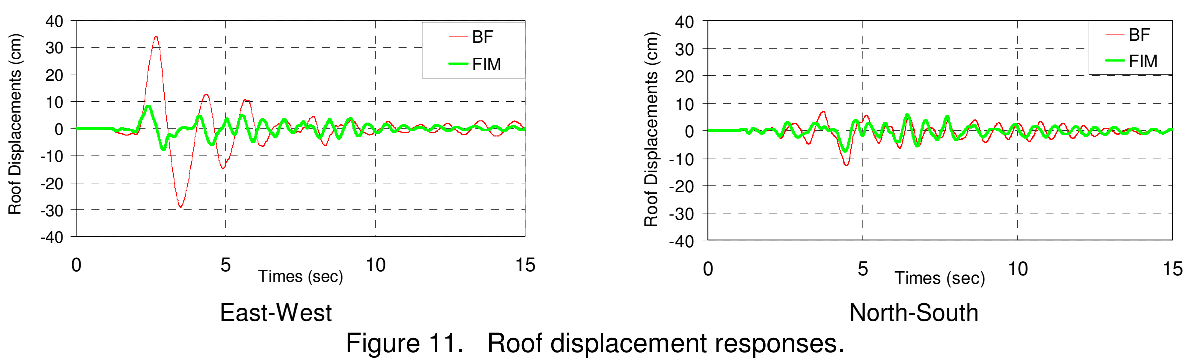

Figure 11. Roof displacement responses.

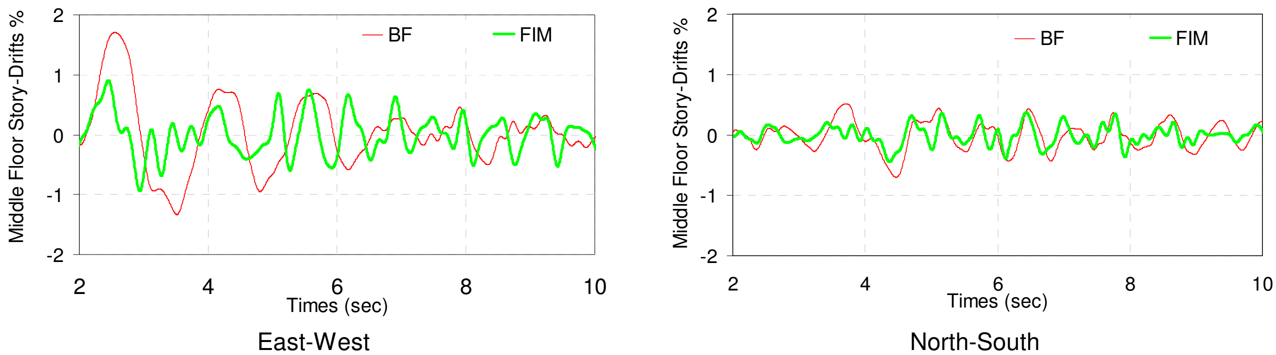

Figure 12. Middle-story drifts ratios (maximum drifts were obtained for this story).

Based on the analysis, maximum displacement responses are estimated for the east-west direction of the building. Lateral Displacements at the roof level in EW and NS directions for bare frame, BF, and frame infilled with masonry wall, FIM, are illustrated in Fig. 11.

Structural responses in Fig. 11 are plotted from the time step 15 seconds up to the time step 30 seconds and in Fig. 12 from the time step 17 second to 25 of the strong motion records in Fig. 10, in order to have discernible curves. Fig. 11 illustrates significant different displacement responses between infilled frame building, type FIM, and bare frame BF. Based on the results, maximum displacement responses, in EW direction, for the type, BF and FIM are estimated as 34 cm and 7 cm respectively. The ratio of maximum displacement response of type BF to that of the FIM is more that 4 times. This may imply the significant effect of the infill walls on the structural performance of Bam Telephone Center building. In other words, a large nonlinear deformations or damages in the building due to the earthquake could be expected, if all the infill masonry walls were out of frame bays. For structural elements of the selected building, it is assumed that drift ratios less than 1% are considered as about linear states. The maximum roof displacement response of 7 cm, for FIM type, is corresponded to a 0.5% drift for the total height of the building, which can be assumed as linear state. However, story drifts should be checked for each floor and column, in order to have this conclusion fulfilled. Fig. 12 shows the time-history story drifts for the two types of categories, BF and FIM at the middle floor, that drifts were maximum. According to the analytical results, story drifts for the category of BF are in the nonlinear states in east-west direction. However, the FIM type, which is expected to be the actual type of the building, performs, in all levels and directions linearly with a maximum story drift ratio of 0.8%. By comparing all the columns story drifts for the FIM type, maximum story drift occurred at the middle floor level with the value of 0.95%. This drift ratio may also be considered as linear drift ratios. Therefore, it might be concluded that the obtained responses are linear as those of the observation. It is also implied that the effect of infill masonry walls would be the main cause of linear performance by the building during the earthquake.

Failure of the infill wall, north side, in the middle floor, with corresponding maximum drift ratio of 0.9% from the analysis

The infill wall, north side, top story, with corresponding maximum drift ratio of 0.1% from the analysis

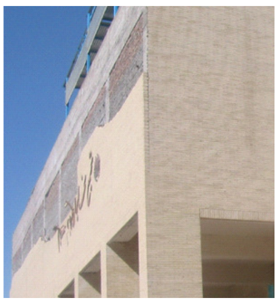

Failure of the infill wall south side top story, with max. drift ratio of 0.15%, however the crash was due to the torsion of the top beam, next to a bay of 13.2 m, with a rotational angle of 0.4%

Out of frame walls, west side, middle floor, with maximum drift ratio of 0.9%

Figure 13. Comparison of the observed damages and results of the nonlinear analysis.

The observed damages on the infill walls are also compared with the results of the nonlinear analysis. For solid brick masonry infill walls, a range of drift ratios of 0.15% to 0.2% for crack drift ratios, a range of 0.6% to 0.7% for drift ratios at maximum loads, and a range of 0.8% to 1% for drift ratios at 80% post-peak load level, are assumed for the sake of comparison, derived from experimental results, (Mehrabi et al. 1996 and Chen Y. H. 2003). The story-drifts ratios for different axes of the building are derived from the analytical results and compared with the observation damages in Fig. 13. Almost in all cases the story-drift ratios are estimated close to the corresponding observed equivalent damage ratios.

Conclusions

A practical analytical process was presented to model infill masonry walls for the purpose of displacement-based analysis of infilled frame structures. An experimental study was carried out to verify the application of the model for infilled frames, common in Japan, which led to a satisfactory agreement between the test data and analytical result. To implement the model in practice, an existing building, damaged by the 2003 Bam-Iran earthquake, was selected and a three-dimensional nonlinear dynamic analysis was implemented to estimate the building responses subjected to the strong motions. Damages observed on the infill walls of the building were compared with the analytical drift ratios, based on the damage rates related to drift ratios, observed previously in experimental studies. As a result, consistent agreements were achieved between damages and the analytical results. A significant effect by infill walls was observed on the structural response of the building. It could be concluded that without the masonry infill walls, the Bam telephone center building would suffer large nonlinear deformations and damages during an earthquake.

Acknowledgments

MEXT, Ministry of Education, Culture, Sport, Science and Technology of Japan sponsored the post-earthquake inspection. Architectural and structural plans and details of the building were provided by the central communication office of Kerman province in Kerman city. Technical supports were provided by Iranian organizations such as Building and Housing Research Center (BHRC), National Disaster Research Institute of Iran (NDRII), and International Institute of Earthquake Engineering and Seismology (IIEES). Thanks are extended to all mentioned supporters who helped this study to be accomplished

References

BHRC, 2004. Strong Motion, *Building and Housing Research Center*, http://www.bhrc.gov.ir/

Chen, Yi-Hsin, 2003. "Seismic Evaluation of RC Buildings Infilled with Brick Walls", *PhD thesis*, National Cheng-Kung Univ., Tainan, Taiwan, in Chinese.

Madan A, Reinhorn AM, Mandar JB, Valles RE, 1997. Modeling of Masonry Infill Panels for Structural Analysis, *Journal of Structural Engineering ASCE* 123(10): 1295-1302.

Mazzoni S., McKenna F., Scott M. H., Fenves, G.L., Jeremic B., 2004. OpenSees Command Language Manual. *PEER Center*, http://opensees.berkeley.edu/

Mehrabi AB, Shing PB, Shuller MP, Noland JL, 1996. Experimental Evaluation of Masonry-Infilled RC Frames, *Journal of Structural Engineering ASCE* 122(3): 228-237.

Moghaddam, H. A., and Dowling, P.J., 1987. The state of the art in infilled frames, *ESEE Research Rep. No 87-2*, Civil Eng. Dept., Imperial College, London.

Mostafaei, H., 2006. Axial-Shear-Flexure Interaction Approach for Displacement-Based Evaluation of Reinforced Concrete Elements, *Ph.D. Thesis*, University of Tokyo, Tokyo

Mostafaei. H. and Kabeyasawa T., 2004. Effect of Infill Masonry Walls on the Seismic Response of Reinforced Concrete Buildings Subjected to the 2003 Bam Earthquake Strong Motion : A Case Study of Bam Telephone Center, *Bulletin of the Earthquake Research Institute Contents 7&9 (3/4),* 133-156.

Mostafaei. H. and Kabeyasawa T., 2004. Investigation and Analysis of Damage to Buildings during the 2003 Bam Earthquake, *Bulletin of the Earthquake Research Institute Contents Contents 7&9 (3/4),* 107-132.

Paulay, T., Priestley M.J.N., 1992. Seismic Design of Reinforced Concrete and Masonry Buildings, *JOHN WILEY & SONS, INC.*

Stafford-Smith and Carter, 1969. A method of analysis for infilled frames, *Proceedings of the Institute of Civil Engineers*, 44, 31-48.